Complex Field-Induced States in Linarite $PbCuSO_4(OH)_2$ with a Variety of High-Order Exotic Spin-Density Wave States

B. Willenberg,[1,2] M. Schäpers,[3] A. U. B. Wolter,[3,*] S.-L. Drechsler,[3] M. Reehuis,[2] J.-U. Hoffmann,[2] B. Büchner,[3,4] A. J. Studer,[5] K. C. Rule,[5] B. Ouladdiaf,[6] S. Süllow,[1] and S. Nishimoto[3,4]

[1]*Institute for Condensed Matter Physics, TU Braunschweig, D-38106 Braunschweig, Germany*
[2]*Helmholtz-Zentrum Berlin für Materialien und Energie, D-14109 Berlin, Germany*
[3]*Leibniz Institute for Solid State and Materials Research IFW Dresden, D-01171 Dresden, Germany*
[4]*Institut für Festkörperphysik, TU Dresden, D-01062 Dresden, Germany*
[5]*The Bragg Institute, ANSTO, Kirrawee DC, New South Wales 2234, Australia*
[6]*Institute Laue-Langevin, F-38042 Grenoble Cedex, France*

(Received 13 August 2015; revised manuscript received 9 November 2015; published 27 January 2016)

Low-temperature neutron diffraction and NMR studies of field-induced phases in linarite are presented for magnetic fields $H\|b$ axis. A two-step spin-flop transition is observed, as well as a transition transforming a helical magnetic ground state into an unusual magnetic phase with sine-wave-modulated moments $\|H$. An effective $\tilde{J}_1$-$\tilde{J}_2$ single-chain model with a magnetization-dependent frustration ratio $\alpha_{\text{eff}} = -\tilde{J}_2/\tilde{J}_1$ is proposed. The latter is governed by skew interchain couplings and shifted to the vicinity of the ferromagnetic critical point. It explains qualitatively the observation of a rich variety of exotic longitudinal collinear spin-density wave, SDW_p, states ($9 \geq p \geq 2$).

DOI: 10.1103/PhysRevLett.116.047202

Recently, frustrated spin chains with ferromagnetic nearest neighbor J_1 (FM-NN) and antiferromagnetic second neighbor J_2 (AFM-NNN) exchange have been discussed in the context of novel states of matter. Close to the saturation field, by tuning the frustration ratio $\alpha = -J_2/J_1$, a sequence of distinct spin-multipolar (MP) phases should develop that contain well-defined phase boundaries; these phases are related to a Tomonaga-Luttinger liquid of p-magnon bound states [1–9]. They compete with exotic longitudinal spin-density wave (SDW_p) correlations, which should prevail in lower magnetic fields.

A proof of existence for spin-MP ordering in real quasi-1D materials is lacking. The FM-AFM chain J_1-J_2 compound $LiCuVO_4$ was considered as a candidate, as it undergoes a transition into an exotic SDW_2 phase above ~8 T [10–13]. A shift of the SDW_2 propagation vector was reported for low fields, together with a transition from long- to short-range magnetic order [13]. These observations were interpreted as a signature of coexisting SDW_2 and bond-nematic order, a view disputed and instead related to a pinned SDW_2 in Refs. [9,14]. Through magnetization and NMR, it was concluded that MP correlations in $LiCuVO_4$ can exist only in a narrow high-field interval of ~1 T width above ~40.5 T [5,15,16].

The issue not resolved in this dispute is the relationship between SDW and MP in the long-range ordered phases appearing in 2D and 3D (in 1D the precursor "phases" overlap [3]). The possibility of homogeneously coexisting SDW_2 and nematic phase and/or phase separation has been suggested for specific conditions and based on pertubative scattering theory [17]. In contrast, only a first-order phase transition was predicted for the same model [9,14]. The situation is far from clear in $LiCuVO_4$. The phase diagram has not been studied in detail due to the high fields required to access it [18]. Further, the influence of defects on the magnetic properties is not well understood [16,19,20]. Thus, a comprehensive study of a clean frustrated FM-AFM spin chain material is desirable to properly define these issues.

A rare example of a frustrated spin-chain system for such studies is the monoclinic linarite (space group $P2_1/m$ [21]). It has been modeled as a $s = \frac{1}{2}$ spin chain with FM-NN $J_1 = -100$ K and AFM-NNN $J_2 = 36$ K [22]. In this J-parameter range the saturation field is about 10 T, allowing full experimental access to the magnetic phase diagram. For a magnetic field $H\|b$ axis the magnetic phase diagram contains five different regions, I (elliptical helix) to V [23–25]. Region V displays very weak thermodynamic signatures, and so it was unclear whether it is a distinct thermodynamic phase. Here, we fully characterize its field-induced phases by means of neutron diffraction (ND) and ^{1}H NMR; we establish not only the magnetic ordering vectors, but also that region V represents a thermodynamic phase. For phase V, we determine the field dependence of the incommensurate (ICM) SDW ordering vector, and we discover complex states that might be understood in terms of phase separation between MP and SDW_p states.

ND was carried out using the single-crystal instrument D10 at the Institute Laue-Langevin, France, and the Wombat instrument at ANSTO, Australia. For the D10 experiment, the sample from a previous study was used [23]. A second linarite crystal from the Grand Reef Mine,

Arizona, was used for the experiment on Wombat. The samples were placed in cryomagnets with maximum field (base temperature) of 6 T (1.7 K) (D10) and 12 T (1.5 K) (Wombat), with the magnetic field applied along the crystallographic b axis. With this setup and a neutron wavelength of 2.36 Å, we were restricted along the b direction to $-0.25 < k < 0.25$ in reciprocal space for the D10 experiment, while for the experiment on Wombat a wavelength of 4.61 Å was used, resulting in an access range $-0.19 < k < 0.19$.

^{1}H-NMR studies were performed for $T < 2.8$ K using a phase-coherent Tecmag spectrometer in combination with a He-flow cryostat. Frequency scans were conducted down to 1.7 K and at external fields $H\|b$ between 1.5 and 7.5 T. We used the same single crystal as for the D10 ND study. All NMR spectra were collected using a $\pi/2 - \tau - \pi$ Hahn spin-echo pulse sequence. The spectra have not been corrected by the tiny spin-spin relaxation time $T_2 \sim 10$ μs.

By ND, scans of $(0, k, 0.5)$ with varying k were performed at 1.7 K for fields up to 6 T. For this temperature the sequence of phases I–III–IV is traversed with increasing field [Fig. 1(a)]. The zero-field magnetic Bragg peak $(0, -0.186, 0.5)$ is also observed at low fields [Fig. 1(b)]. For an increasing magnetic field, at the boundary to phase III, a second commensurate (CM) Bragg peak appears at $(0, 0, 0.5)$, corresponding to spins coupled parallel along the a and b axes and antiparallel along c. In the field range 2.60 to 2.95 T both peaks coexist, while for higher fields (in phase IV) only the commensurate Bragg peak remains. This scenario is fully consistent with our NMR experiments (see Ref. [26]), showing that a phase separation into two competing spin structures occurs in phase III.

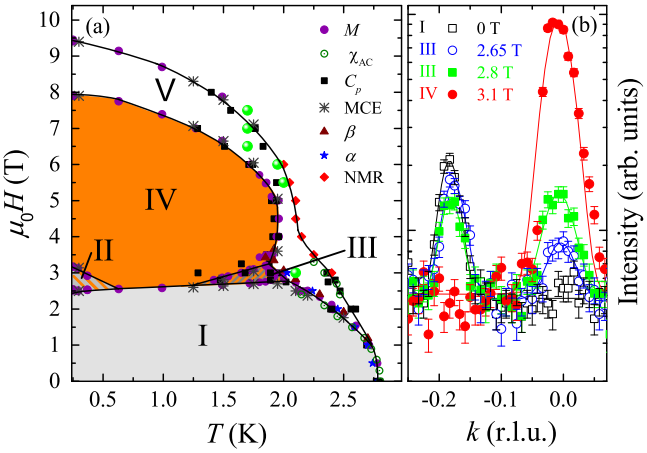

FIG. 1. (a) Phase diagram of linarite with $H\|b$. For a description of the phases I–V, see the text. Red diamonds mark new transition temperatures into phase V. Green balls indicate the (H,T) points of Fig. 3. (b) Neutron scattering scans along k at 1.7 K as function of the magnetic field, crossing from phase I via III into IV. Solid lines are Gaussian fits for peak position determination.

To determine the magnetic structure with the propagation vector $\boldsymbol{k} = (0, 0, 0.5)$ of phase IV, the intensity of 33 magnetic Bragg peaks (20 of which were inequivalent) was measured at 4 T by ND. A refinement of the data ($R_F = 9.5\%$) using FullProf [28] reveals that the spins are lying in the ac plane, with an angle of $-27°$ off the a axis, the same as one of the spin components of the phase-I helix [23]. From the refinement, an ordered moment of $0.79(1)\mu_B$ per Cu atom is derived. Similar refinements at 5.5 T (20 inequivalent Bragg peaks) yield the same spin structure with a moment of $0.73(2)\mu_B$ per Cu atom ($R_F = 12.5\%$). The decrease of the AFM moment with the field, and the observation of small field-induced FM contributions on top of nuclear Bragg peaks, reflects the development of field-induced spin polarization.

For the determination of the spin structures in phase III, two sets of magnetic Bragg peaks $(hkl)_M$ were collected at 2.8 T using the relation $(hkl)_M = (hkl)_N \pm \boldsymbol{k}$. For the ICM structure, the propagation vector $\boldsymbol{k} = (0, 0.186, 0.5)$ was used; for the CM structure, $\boldsymbol{k} = (0, 0, 0.5)$. The CM structure in phase III is refined using 15 peaks (14 of which were inequivalent) with the phase-IV spin model. The refinement of 18 inequivalent Bragg peaks of the ICM structure yields a circular helix structure ($R_F = 14.5\%$), where the moments of $0.64(2)\mu_B$ lie roughly in the bc plane.

In the related chain systems $LiCuVO_4$ and $LiCu_2O_2$, applying a magnetic field rotates the normal of the helical structure parallel to the field. Here, such a spin flop of the helix into the ac plane is prohibited by the monoclinic angle β. Instead, in phase III the spins start to flop into the ac plane, forming a collinear spin arrangement, while a coexisting helical phase is retained. The fact that in phase III a circular helix (a spinning plane in the bc plane) replaces the elliptical helix reflects that for the latter it is energetically costly to keep the large moment axis aligned along the field direction. For larger fields all spins are flopped into the ac plane, forming the collinear phase IV.

Next, we have performed ND via k scans through region V [Fig. 2(a)]. Surprisingly, and in spite of the weak signatures defining this region in thermodynamic measurements [23,24], we observe magnetic Bragg peaks of the same width as the nuclear peaks. These peaks are even observed in the intermediate field regime ~4 T, where no anomalies were detected in thermodynamic measurements [24]. This implies that region V is a distinct and highly unusual thermodynamic phase. For a magnetic structure determination, a set of 8 inequivalent Bragg peaks was collected at 6 T. A refinement yields a sine-wave-modulated structure, with the spins aligned parallel to the b axis ($R_F = 7\%$). Surprisingly, the SDW magnetic moment amplitude is only $0.44(1)\mu_B$, which is much smaller than the magnetic moments measured in phase I and IV. Further, the propagation vector $(0, -k, 0.5)$ shifts in

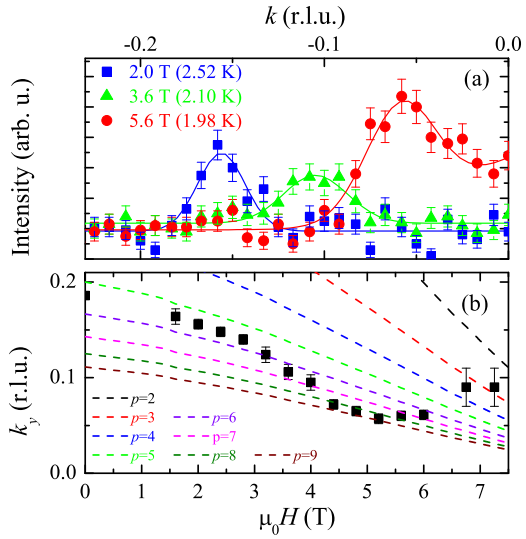

FIG. 2. (a) The magnetic Bragg peak position $(0, k, 0.5)$ shift in phase V. (b) Field dependence of the propagation vector in phase V compared to the 1D model SDW_p states with $2 \leq p \leq 9$. Theory lines include the magnetization obtained from $M(H,T)$ scans [24].

k with the field, as shown in Fig. 2. A schematic view summarizing the different magnetic structures of linarite for $H \| b$ is given in the Supplemental Material [26].

The sine-wave-modulated structure with moments along the field direction, together with the shift of the k value, reminds us of the prediction of the longitudinal collinear SDW within the hard-core boson approximation [1,3,8], where the shift depends on the number of bound magnons p in the coexisting or neighboring MP phase,

$$\frac{k_y d}{\pi} = \frac{(1 - M/M_S)}{p}. \tag{1}$$

Here, d denotes the distance of neighboring Cu spins along the b axis, and M_S is the saturation magnetization [29]. To compare Eq. (1) with the situation for linarite, the curves with various p values are included in Fig. 2(b). Surprisingly, at first glance no agreement is found over a wide field range between the experimentally observed evolution of k_y and the theoretical prediction for a single chain with a fixed value of p (see also discussion below).

Static magnetic order in phase V is also observed by NMR. Frequency scans were performed every 0.5 T in the field range 3–7.5 T at different temperatures. At 2.8 K, a paramagnetic signal is observed that is composed of two almost overlapping lines from two inequivalent ^{1}H sites [25]. For fields ≤ 6 T, upon lowering T below a critical value T_V, the spectrum develops horn-shaped NMR characteristics, that is, two distinct peaks with a finite intensity in between [Figs. 3(a)–3(c)]. This can be accounted for by the SDW structure with a magnetic component only along the b direction (compare $LiCuVO_4$ [16]). The transition temperatures derived from NMR define the phase boundary in the field range 3.5–6 T, where no transition has been detected in thermodynamic quantities [23,24]. Our findings imply that phase V encloses all other magnetic phases [see Fig. 1(a)].

Increasing the field to above 6 T within phase V [Figs. 3(d)–3(e)] produces a transfer of spectral weight from the horn-shaped structure to a broadened two-peak structure appearing in the middle of the SDW pattern. The shift of the latter with an increasing field follows the shift of the paramagnetic polarized NMR signal close to saturation. Qualitatively, this implies the presence of two different local environments in the sample, viz., a phase separation occurs. In part of the sample there is SDW ordering, while the regions of the sample exhibiting the broadened two-peak structure show no static magnetic order. Based on the 1D calculations given in Refs. [1–3], for 2D or 3D coupled frustrated spin chains, a field-induced transition from the SDW_p into a p-MP phase could be expected in high fields. This transition should appear as one from a magnetically long-range ordered state into one without static dipolar long-range order. Hence, we suggest that the phase separation observed in phase V is related to the transition from a SDW_p phase into one with dominant MP character in a quasi-1D material.

To discuss our experimental results, we study weakly coupled J_1-J_2 chains in a magnetic field H along the z axis using the density-matrix-renormalization group (DMRG) method. The Hamiltonian reads as

$$\hat{H} = J_1 \sum_{l,i} \mathbf{S}_{l,i} \cdot \mathbf{S}_{l,i+1} + J_2 \sum_{l,i} \mathbf{S}_{l,i} \cdot \mathbf{S}_{l,i+2} + H \sum_{l,i} S^z_i + J_{\mathrm{ic}} \sum_{l,l',i,i'} \mathbf{S}_{l,i} \cdot \mathbf{S}_{l',i'}, \tag{2}$$

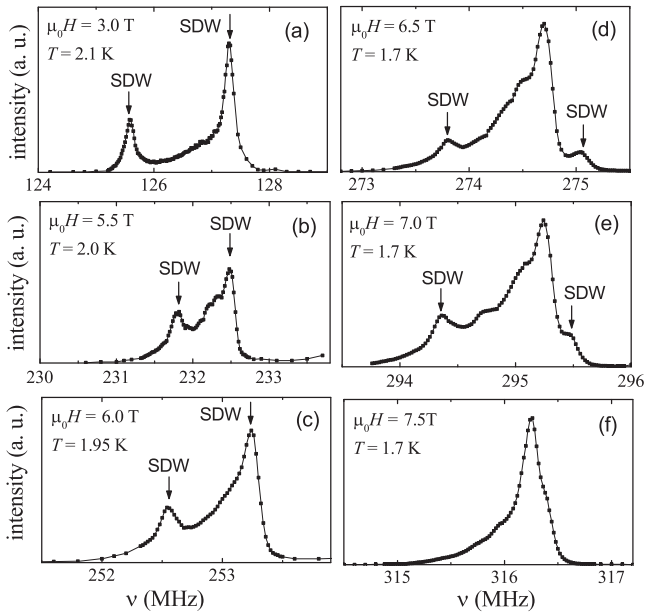

FIG. 3. ^{1}H-NMR spectra of linarite in phase V (a)–(e) and in the paramagnetic polarized state at 7.5 T (f) close to saturation.

where $\mathbf{S}_{l,i}$ is a spin-$\frac{1}{2}$ operator at site i in chain l and $J_{\rm ic}$ is a diagonal interchain coupling [see Fig. 4(a)]. As shown above, the ICM propagation vector along the chain is $k_y = 0.186\pi$ at $H = 0$; however, a single J_1-J_2 chain with $\alpha = J_2/|J_1| = 0.36$ gives $k_y \approx 0.367\pi$. This discrepancy can be resolved by taking a specific diagonal $J_{\rm ic} \approx 10$ K $= 0.1|J_1|$. Theoretically, the propagation vector in the single J_1-J_2 chain is found from the maximum position of the static spin-structure factor $S(k)$. Because of strong quantum fluctuations and the resulting absence of static magnetic order in 1D with only short-range couplings, the propagation vector cannot be found from $\langle S_i^z \rangle$. As a precursor, however, the former reflects nevertheless the SDW modulations (induced by the coupling to neighboring chains in 2D and 3D) that we are looking for here. This maximum position of $S(k)$ is reduced by decreasing α, and it approaches 0 at the FM critical point $\alpha_c = 1/4$. Such a reduction of the propagation vector is also realized by increasing $J_{\rm ic}$ at fixed α for a system of coupled chains [30]. It is thus interpreted that the interchain coupling reduces the value of α.

Near the FM critical point $\alpha_c = 1/4$, higher ($p > 4$) MP states together with a field-theory-predicted panoply of novel phases could appear at high fields [31]. Since there are many degenerate low-lying states near $\alpha_c = 1/4$, a single chain is more convenient than coupled chains to maintain the accuracy of our DMRG calculations. Therefore, we first performed a mapping from two coupled J_1-J_2 chains with $\alpha = 0.36$ and $J_{\rm ic} = 0.1|J_1|$, and with periodic perpendicular boundary conditions, onto an effective single $\tilde{J}_1$-$\tilde{J}_2$ chain with $\alpha_{\rm eff} = -\tilde{J}_2/\tilde{J}_1 = \alpha_{\rm eff}(\alpha, M/M_s, J_{\rm ic}/|J_1|)$. For a wide range of the magnetization M/M_s the values of $\alpha_{\rm eff}$ were estimated by fitting the dynamical spin-structure factors $S(\mathbf{q}, \omega)$. An example is shown in Fig. 4(b) (for details see Ref. [26]). The estimated values of $\alpha_{\rm eff}$ are plotted vs M/M_s in Fig. 4(c); note the vicinity to α_c.

Next, we found the number of bound magnons p for a given α by calculating the binding energy of a p-magnon bound state near the saturation field [for lower fields, see Supplemental Eq. (S5) and below therein [26]], which is defined as

$$E_b(p) = \frac{1}{p}[E(S_z = S_{\rm max} - p) - E(S_z = S_{\rm max})] - [E(S_z = S_{\rm max} - 1) - E(S_z = S_{\rm max})], \quad (3)$$

where $E(S_z = S)$ is the ground-state energy with the z component of the total spin $S_z = S$, and $S_z = S_{\rm max}$ corresponds to the fully polarized state. When the largest value of $E_b(p)$ (> 0) is given by $p = p_{\rm max}$, we can prove that the $p_{\rm max}$-magnon bound state is the most stable state, whereas if $E_{\rm b}(p) < 0$ for all p values, no low-energy magnon bound state exists. The results are shown in Fig. 4(c). According to Refs. [1–3], the value of p increases as $\alpha_{\rm eff}$ approaches 1/4

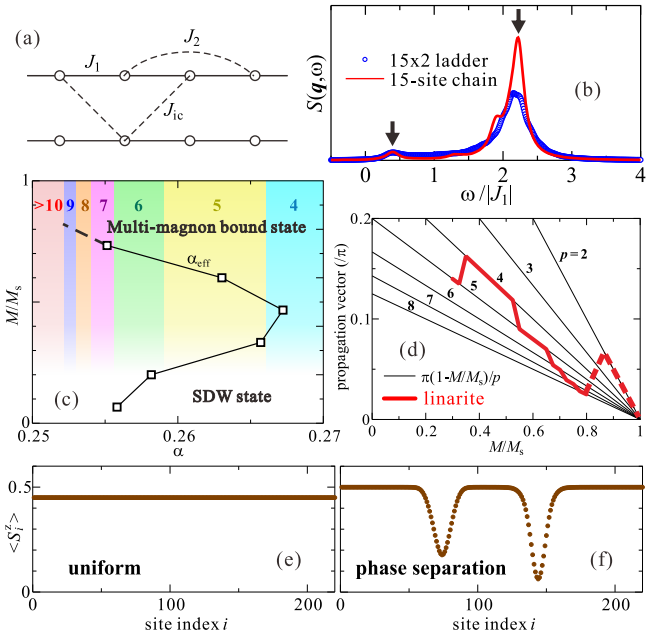

FIG. 4. (a) Lattice model of weakly coupled J_1-J_2 chains. (b) Fitting of $S(\mathbf{q}, \omega)$ at $M/M_s = 0.2$, between $\mathbf{q} = (\pi, \pi)$ for two coupled chains with $\alpha = 0.36$, $J_{\rm ic} = 0.1|J_1|$, and $q = \pi$ for a single chain with $\alpha_{\rm eff} = 0.257$. (c) Phase diagram of the multi-magnon bound states and the estimated effective frustration ratio $\alpha_{\rm eff}$ for linarite. (d) Suggested propagation vector using (c). (e),(f) Local spin densities $\langle S_i^z \rangle$ at $\alpha_{\rm eff} = 0.26$ and $M/M_s = 0.95$ for (e) periodic and (f) open chains.

and the region of $\alpha_{\rm eff}$ becomes narrower for larger p. From the relation between p and $\alpha_{\rm eff}$, we suggest that the propagation vector of linarite evolves similarly to that shown in Fig. 4(d); this is based on calculations within our effective 1D model, in semiquantitative agreement with the experimental data [Fig. 2(b)]. For a brief discussion of the dashed part of the red line related to $p = 2$ obtained within an analogous xyz-anisotropic Heisenberg model, see Ref. [26].

The phase separation observed at high field may be attributed to the low effective frustration ratio $\alpha_{\rm eff} \approx 1/4$. This means that the FM state is almost degenerate to other lower spin states. As an illustration, the local spin densities $\langle S_i^z \rangle$ with periodic and open boundaries at $M/M_s = 0.95$ for $\alpha_{\rm eff} = 0.26$ are plotted in Figs. 4(e) and 4(f), respectively. A uniform distribution is naturally expected for periodic chains, whereas interestingly, a phase separation into partial polarized and unpolarized phases occurs near open chain ends and possibly also near strong-enough impurities in the bulk.

To conclude, linarite exhibits a field-induced behavior generic for a FM-NN/AFM-NNN frustrated chain system. In addition, a two-step spin-flop transition is present for external magnetic fields applied along the b axis. Further, a longitudinal sine-wave-modulated spin-structure phase with a field-dependent propagation vector encloses the

other ordered phases. To the best of our knowledge, we report the first observation of several exotic (for Heisenberg spin-1/2 systems) collinear longitudinal SDW_p states, reaching even $p = 9$; we accomplish this by changing the external field. We believe that this result is related to the appropriate bare value of α and the strong-enough skew interchain coupling. Considered in general, linarite appears to be a good candidate to show MP behavior. A more detailed and comprehensive study, including its exotic SDW_p states and their interplay with field-induced phase separation and exchange anisotropy, provides a challenge for future work.

Our work has been supported by the DFG under Contracts No. WO 1532/3-1 and No. SU 229/9-1. We acknowledge fruitful discussions with W. Brenig, A. Läuchli, U. Rößler, N. Shannon, O. Starykh, H. Tsunetsugu, and M. Zhitomirsky. We thank G. Heide and M. Gäbelein from the Geoscientific Collection in Freiberg for providing the linarite crystal.

*a.wolter@ifw-dresden.de

[1] L. Kecke, T. Momoi, and A. Furusaki, Phys. Rev. B **76**, 060407 (2007).
[2] T. Hikihara, L. Kecke, T. Momoi, and A. Furusaki, Phys. Rev. B **78**, 144404 (2008).
[3] J. Sudan, A. Lüscher, and A. M. Läuchli, Phys. Rev. B **80**, 140402 (2009).
[4] F. Heidrich-Meisner, I. P. McCulloch, and A. K. Kolezhuk, Phys. Rev. B **80**, 144417 (2009).
[5] M. E. Zhitomirsky and H. Tsunetsugu, Europhys. Lett. **92**, 37001 (2010).
[6] S. Nishimoto, S.-L. Drechsler, R. Kuzian, J. Richter, and J. van den Brink, J. Phys. Conf. Ser. **400**, 032069 (2012).
[7] S. Nishimoto, S.-L. Drechsler, R. Kuzian, J. Richter, and J. van den Brink, Phys. Rev. B **92**, 214415 (2015).
[8] M. Sato, T. Hikihara, and T. Momoi, Phys. Rev. Lett. **110**, 077206 (2013).
[9] O. A. Starykh and L. Balents, Phys. Rev. B **89**, 104407 (2014).
[10] B. J. Gibson, R. K. Kremer, A. V. Prokofiev, W. Assmus, and G. J. McIntyre, Physica (Amsterdam) **350B**, E253 (2004).
[11] N. Büttgen, H.-A. Krug von Nidda, L. E. Svistov, L. A. Prozorova, A. Prokofiev, and W. Aßmus, Phys. Rev. B **76**, 014440 (2007).
[12] N. Büttgen, W. Kraetschmer, L. E. Svistov, L. A. Prozorova, and A. Prokofiev, Phys. Rev. B **81**, 052403 (2010).
[13] M. Mourigal, M. Enderle, B. Fåk, R. K. Kremer, J. M. Law, A. Schneidewind, A. Hiess, and A. Prokofiev, Phys. Rev. Lett. **109**, 027203 (2012).
[14] O. Starykh, Rep. Prog. Phys. **78**, 052502 (2015).
[15] L. Svistov, T. Fujita, H. Yamaguchi, S. Kimura, K. Omura, A. Prokofiev, A. Smirnov, Z. Honda, and M. Hagiwara, Pis'ma v Zh. Èksper. Teoret. Fiz. **93**, 24 (2011) [JETP Lett. **93**, 21 (2011)].
[16] N. Büttgen, K. Nawa, T. Fujita, M. Hagiwara, P. Kuhns, A. Prokofiev, A. P. Reyes, L. E. Svistov, K. Yoshimura, and M. Takigawa, Phys. Rev. B **90**, 134401 (2014).
[17] H. Ueda and K. Totsuka, arXiv:1406.1960.
[18] N. Büttgen, P. Kuhns, A. Prokofiev, A. P. Reyes, and L. E. Svistov, Phys. Rev. B **85**, 214421 (2012).
[19] L. A. Prozorova, S. S. Sosin, L. E. Svistov, N. Büttgen, J. B. Kemper, A. P. Reyes, S. Riggs, A. Prokofiev, and O. A. Petrenko, Phys. Rev. B **91**, 174410 (2015).
[20] A. Prokofiev, I. Vasilyeva, V. Ikorskii, V. Malakhov, I. Asanov, and W. Assmus, J. Solid State Chem. **177**, 3131 (2004).
[21] H. Effenberger, Mineralogy and petrology **36**, 3 (1987).
[22] A. U. B. Wolter, F. Lipps, M. Schäpers, S.-L. Drechsler, S. Nishimoto, R. Vogel, V. Kataev, B. Büchner, H. Rosner, M. Schmitt, M. Uhlarz, Y. Skourski, J. Wosnitza, S. Süllow, and K. C. Rule, Phys. Rev. B **85**, 014407 (2012).
[23] B. Willenberg, M. Schäpers, K. C. Rule, S. Süllow, M. Reehuis, H. Ryll, B. Klemke, K. Kiefer, W. Schottenhamel, B. Büchner, B. Ouladdiaf, M. Uhlarz, R. Beyer, J. Wosnitza, and A. U. B. Wolter, Phys. Rev. Lett. **108**, 117202 (2012).
[24] M. Schäpers *et al.*, Phys. Rev. B **88**, 184410 (2013).
[25] M. Schäpers, H. Rosner, S.-L. Drechsler, S. Süllow, R. Vogel, B. Büchner, and A. U. B. Wolter, Phys. Rev. B **90**, 224417 (2014).
[26] See Supplemental Material at http://link.aps.org/supplemental/10.1103/PhysRevLett.116.047202, which also includes Refs. [13,22,25,27,31], for detailed information about the NMR spectra in the different phases as well as for a summary of the magnetic structures in phases I, III, IV, and V. Further information about the mapping procedure of two coupled J_1-J_2, J_{ic} chains are also given.
[27] W. E. A. Lorenz, R. O. Kuzian, S.-L. Drechsler, W.-D. Stein, N. Wizent, G. Behr, J. Málek, U. Nitzsche, H. Rosner, A. Hiess, W. Schmidt, R. Klingeler, M. Loewenhaupt, and B. Büchner, Europhys. Lett. **88**, 37002 (2009).
[28] J. Rodríguez-Carvajal, Physica (Amsterdam) **192B**, 55 (1993).
[29] Note that for linarite and $LiCuVO_4$, the lattice constant $b = 2d$ due to alternating side groups.
[30] S. Nishimoto, S.-L. Drechsler, R. Kuzian, J. Richter, J. Málek, M. Schmitt, J. van den Brink, and H. Rosner, Europhys. Lett. **98**, 37007 (2012).
[31] L. Balents and O. A. Starykh, arXiv:1510.07640.